

On the importance of the choice of wind stress forcing to the modeling of the Mediterranean Sea circulation

Paul G. Myers and Keith Haines

Department of Meteorology, University of Edinburgh, Edinburgh, Scotland, United Kingdom

Simon Josey

James Rennell Division for Ocean Circulation, Southampton Oceanography Centre, Southampton England, United Kingdom

Abstract. A $1/4^\circ$ degree ocean general circulation model is used to examine the role that four different wind stress climatologies play on the circulation of the Mediterranean. The wind stress climatologies examined are those derived from numerical weather prediction models (National Meteorological Center (NMC) and European Centre for Medium-Range Weather Forecasts (ECMWF)) and one based on observations (Southampton Oceanography Centre (SOC)). Significant differences exist between the wind climatologies over the Mediterranean and in the response of an ocean general circulation model forced by the different climatologies. Excessive coastal upwelling/downwelling is found to be associated with the extreme zonal nature of one of the climatologies. Surface circulation differences include the position and penetration of the Mid-Mediterranean Jet into the Levantine, the Ionian, and the Tyrrhenian circulations. Significant differences exist in the pathways for dispersal of Levantine Intermediate Water. Under the SOC forcing, there is a reduction in Eastern Mediterranean Deep Water formation in the Southern Adriatic, compensated by the production of intermediate or deep water in the Aegean. The ECMWF climatology is found to be associated with much more cyclonic doming in the Gulf of Lions, leading to better formation of Western Mediterranean Deep Water.

1. Introduction

One of the most basic ways in which the atmosphere drives the ocean is through the wind stresses applied to the ocean's surface. Although directly felt only in the thin upper Ekman layer, the wind can nevertheless play a role in driving the major ocean currents. Even the deep circulation, which is generally thought to be part of the thermohaline circulation, and thus buoyancy controlled, can be affected by the winds, for example, through the transport of water masses to deep water formation sites, preconditioning of convection by the doming of isopycnals, trapping of water in deep water formation sites, and the modification of the surface fluxes.

The Mediterranean is a small marginal sea located between Europe and Africa (Figure 1). Despite its marginal nature it is an important basin because it possesses an active thermohaline circulation, with deep convection and water mass formation. The small spatial

scales and short timescales associated with this thermohaline circulation make it ideal for study. Over the last decade or so many advances have been made in the observation and modeling of this basin.

Together with the surface buoyancy fluxes and the inflow through the Strait of Gibraltar, wind stress drives the Mediterranean circulation. *Pinardi and Navarra* [1993] suggest that the buoyancy and wind forcing may both act on seasonal timescales and play a key role in the transport and dispersal of water masses. A number of modeling studies have used different wind stresses calculated either from in situ observations or from the analyses of weather prediction centers. *Stanev et al.* [1989] used a wind stress computed from seasonal pressure data using an Ekman boundary layer approximation. *Pinardi and Navarra* [1993] used the *Hellerman and Rosenstein* [1983] climatology to examine the wind-driven general circulation of the Mediterranean. *Heburn* [1994] used both *Hellerman and Rosenstein* [1983] and a hybrid form from the European Centre for Medium-Range Weather Forecasts (ECMWF) and showed that wind plays a significant role in forcing the circulation. *Zavatarelli and Mellor* [1995] use the climatology of *May* [1982], an observationally based climatology, while

Copyright 1998 by the American Geophysical Union.

Paper number 98JC00784.
0148-0227/98/98JC-00784\$09.00

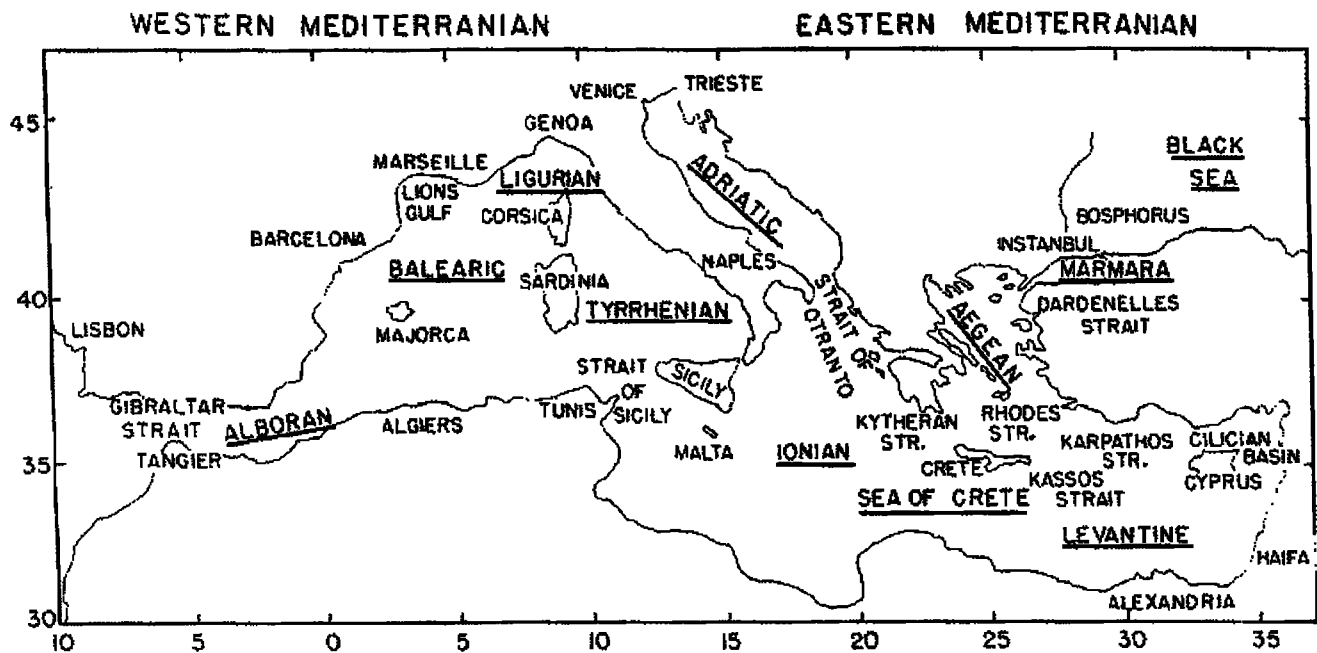


Figure 1. A map detailing some of the main Mediterranean locations mentioned in this paper (taken from *Malanotte-Rizzoli and Hecht* [1988]).

Roussenov et al. [1995] use a modified wind field based on the output from the National Meteorological Center (NMC) weather forecast model. The Mediterranean Models Evaluation Experiment (MEDMEX) [*Beckers et al.*, 1996] used the ECMWF wind stresses as part of an intercomparison project examining five models of the Mediterranean and suggested that one of the reasons why the different models have similar general circulations with different hydrography is the choice of identical wind stress [*Beckers et al.*, 1997]. All of these studies find that the wind (and especially its seasonality) plays a major role in driving the circulation of the Mediterranean. However, thus far no systematic study has been made upon the effect that the choice of the wind stress climatology has on the circulation, using the same model.

In a recent series of papers, *Haines and Wu* [1995] and *Wu and Haines* [1996,1998] examined the dispersal of Levantine Intermediate Water (LIW) in a general circulation model of the entire Mediterranean. They found that the LIW plays a key role in the basin's thermohaline circulation, providing salt to the deep water formation sites, as well as for export through Gibraltar into the Atlantic. In all their experiments they used the annual wind climatology calculated by *Roussenov et al.* [1995] based on the National Meteorology Center model; this climatology when used here is referred to as NMC-R.

The analyzed 10-m wind stress output from ECMWF, as chosen for the Mediterranean Models Evaluation Experiment (MEDMEX) [*Beckers et al.*, 1996], is also used here. A third wind climatology is one that has

been produced recently at the Southampton Oceanography Centre (SOC) using in situ observations [*Josey et al.*, 1996]. Being directly derived from measurements this in situ climatology has many features in common with that of *May* [1982]. We also use winds directly from the NMC reanalysis which will expose some of the biases introduced in the NMC-R fields. Although the time periods covered by the different climatologies are not identical, which can lead to differences, these are less significant compared with those due to the different origin, analysis, and processing procedures; see section 2. The goals of our study are to (1) examine the importance of the choice of wind stress forcing for model response and (2) provide the necessary information that would allow one to determine whether differences between model circulations found in past studies can be associated with the choice of wind stress forcing.

The climatologies are described in more detail in section 2. The model used and the experiments performed are presented in section 3. Section 4 consists of an examination of the model diagnosed fluxes while a detailed examination of the circulation changes related to the use of the different wind stress climatologies is presented in section 5. A discussion and a summary are given in section 6.

2. Wind Stress Climatologies

The NMC-R climatology used in our study was that derived by *Roussenov et al.* [1995] from twice-daily 1000-hPa operational analyses of winds from the NMC weather prediction model (on a $1^\circ \times 1^\circ$ grid) covering the

period January 1980 to December 1988. In their analysis the model wind speed components and sea surface and air temperatures were used to calculate the surface stress according to the bulk formula

$$(\tau_x, \tau_y) = \rho_a C_D |\mathbf{w}| (w_x, w_y) \quad (1)$$

where τ and w are the wind stress and speed, respectively, and subscripts x and y denote zonal and meridional components. $\rho_a = 1.2 \text{ kg m}^{-3}$ is the surface air density, and C_D is the drag coefficient. The latter was estimated using the simple polynomial approximation of *Hellerman and Rosenstein* [1983], in which the air-sea temperature difference is taken as a measure of atmospheric stability. However, as discussed by *Harrison* [1988], the Hellerman and Rosenstein approximation is widely believed to overestimate the true drag coefficient, which is now thought to be better determined with schemes such as those of *Smith* [1980] and *Large and Pond* [1981] that take lower values for the neutral drag coefficient and include a more complete treatment of the atmospheric stability. *Harrison* found that the *Large and Pond* drag coefficient values were typically 20% smaller than those obtained using the Hellerman and Rosenstein scheme. Hence, in an attempt to determine the importance of this difference in C_D we performed a secondary experiment with the NMC-R wind stress fields multiplied by 0.8, to simulate the smaller drag coefficient. However, the precise magnitude of the wind stress field is of secondary importance, and it is the directional dependence that dominates the model's circulation response. The direction is set both by the fact that the analysis is based upon the 1000-hPa level and by the atmosphere model's normalization scheme.

The ECMWF climatology is based on 7 years (1986-1992) of reanalyzed monthly mean wind stress fields on a $1.125^\circ \times 1.125^\circ$ grid; the wind stress fields, in turn, have been computed using four times daily wind analyses from the ECMWF weather prediction model. The stresses are computed from the model winds using the bulk formula, (1), with the drag coefficient C_D , on the basis of the scheme of *Large and Pond* [1981]. The winds are corrected from 30 m, the bottom model layer, to 10 m using the ECMWF's boundary layer model.

The third set of wind stress fields is taken from the new Southampton Oceanography Centre (SOC) air-sea heat and momentum flux climatology [*Josey et al.*, 1996]. The climatology has been calculated using ship meteorological reports contained in the COADS1a data set [*Woodruff et al.*, 1993], which covers the period 1980-1993, blended with additional metadata describing observational procedure (height of observing platforms, etc.) from the WMO47 list of ships [*World Meteorological Organization*, 1994], which allows corrections to be made for various observational biases. The wind stress has again been calculated using (1) but in the SOC analysis the drag coefficient relationship suggested by *Smith* [1980] was employed. We note that the *Smith*

[1980] formulation for C_D is in good agreement with the results of a recent analysis of an extensive set of wind stress measurements made under open ocean conditions [*Yelland et al.*, 1998]. The direct NMC experiment is performed using winds taken from the NMC reanalysis and converted to stresses using the same bulk formula as used for the NMC-R experiment above. Daily data from 1980 to 1988 are used, from the 10 m level, interpolated from a $1.875^\circ \times 1.9^\circ$ grid.

The climatological monthly mean wind stress fields for each of the data sets considered are shown in Figure 2 for January and Figure 3 for July. Daily values of the wind stress components are calculated for use in the model from the monthly averages using linear interpolation for all climatologies.

The stress patterns for the ECMWF and SOC climatologies are similar in January, with a strong cyclonic circulation over the Levantine, a vigorous Mistral, and generally southeastward flow, the magnitude of the stress being generally slightly greater in the SOC

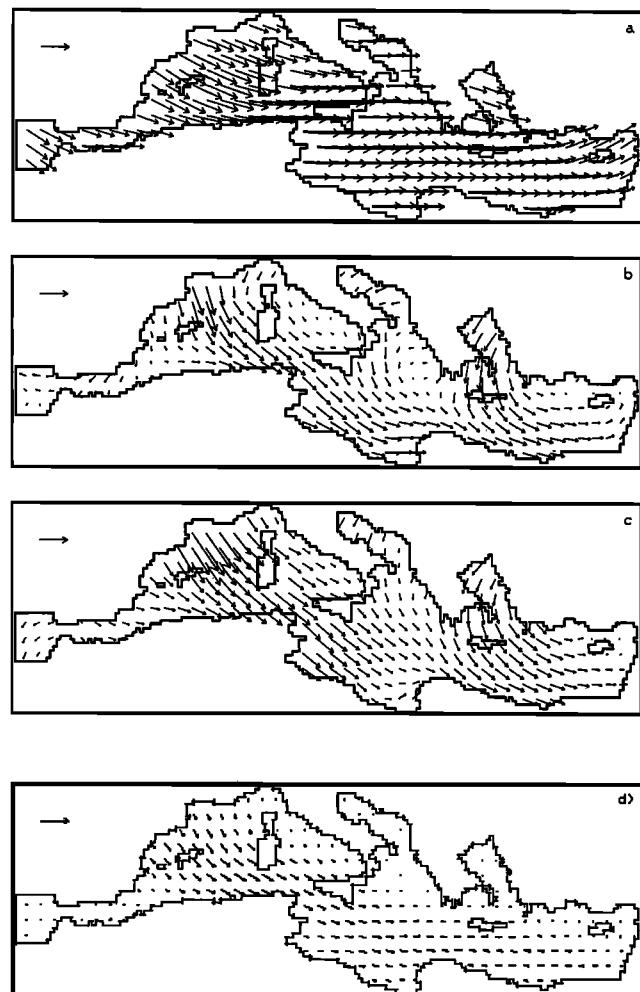


Figure 2. Wind stress climatologies for January: (a) NMC-R, (b) ECMWF, (c) SOC, and (d) NMC. The scale arrow in the top left-hand corner of each plot represents a vector of magnitude 0.1 N m^{-2} .

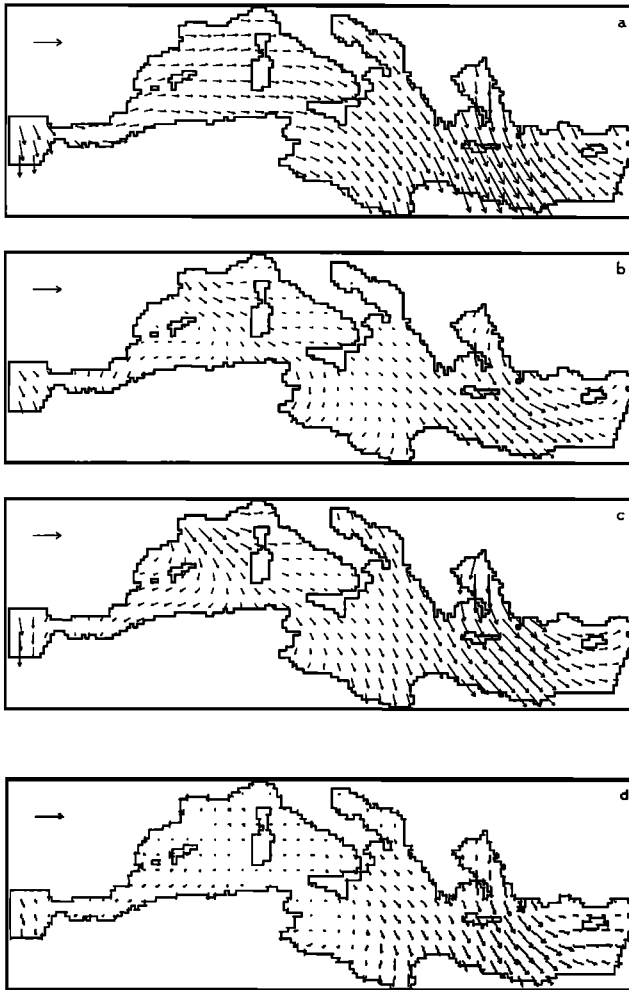


Figure 3. Wind stress climatologies for July: (a) NMC-R, (b) ECMWF, (c) SOC, and (d) NMC. The scale arrow in the top left-hand corner of each plot represents a vector of magnitude 0.1 N m^{-2} .

fields (Table 1). Small-scale differences are most noticeable in the Adriatic, north Ionian, Tyrrhenian, and Alboran Seas. In particular, in the Alboran Sea the ECMWF stresses are northeasterly, while the SOC values are northwesterly and this difference may influence

the ability of the model to reproduce the double-gyre structure in this region (see section 5.1). In contrast, the NMC-R climatology has a very different circulation pattern, with mainly zonal flow over the bulk of the Mediterranean and a weak Mistral. The NMC stresses are closer to the ECMWF and SOC climatologies in the western Mediterranean during winter, with a vigorous Mistral and significantly less zonal flow. However, the stresses are considerably weaker (Table 1). The NMC flow in the eastern Mediterranean is also weaker than NMC-R and does retain the zonal nature.

In July the ECMWF and SOC climatologies are again in broad agreement, with the SOC stresses being slightly stronger. The NMC-R field is now less zonal and in closer agreement with the other two over the eastern Mediterranean, which lies under a northwesterly flow. The flow is noticeably weaker in the ECMWF climatology over the northern Ionian and Adriatic. The NMC-R field remains predominantly zonal over the western Mediterranean, while an anticyclonic circulation in the region west of Sardinia is evident in the other two data sets. The July NMC fields are similar to the ECMWF stresses (Table 1), again being less zonal than the NMC-R stresses in the western basin.

Roussenov et al. [1995] noted the unusual zonality in the NMC-R fields relative to an earlier climatology compiled by *Hellerman and Rosenstein* [1983], which was based on ship observations between 1870 and 1976, and suggested that it was due to the short length of the time series used in their analysis. However, this is clearly not the cause, as the ECMWF and SOC fields presented here are also based on relatively short time series and yet exhibit the range of features seen in the longer-term study. Some of the zonality, particularly in the eastern basin in winter, is due to the NMC analysis, since Figures 2a and 2d are both quite zonal. However, the use of a simple scalar averaging technique employed by *Roussenov et al.* [1995] tends to increase zonality. The NMC-R monthly mean wind stresses were generated from six hourly values by separately averaging the wind stress magnitude and direction. In contrast, a vector average of the wind stress values (i.e., averaging

Table 1. Measure of the Wind Stress, Spatially Averaged Over the Entire Model Domain, for Each Climatology

Experiment	January		July	
	X Component	Y Component	X Component	Y Component
NMC-R	9.65	-0.90	2.96	-2.94
ECMWF	2.04	-2.13	1.23	-1.32
SOC	3.04	-2.66	1.68	-2.38
NMC	1.36	-0.51	0.93	-1.41

Both the X and Y components of the averaged stress (in 10^{-2} N m^{-2}) are given for two representative months, January and July.

the zonal and meridional components separately) was taken when generating the ECMWF and SOC fields. The scalar averaging method can result in fields that are quite different from those obtained with the more appropriate vector mean in regions where there are significant directional variations over the averaging period, tending to generate strongly zonal fields in the case of the Mediterranean. Despite the potential problems introduced by the scalar averaging technique we have included the NMC-R fields in our study as they have already been widely employed elsewhere in the literature and our aim is to highlight the differences that arise when modeling the Mediterranean as a result of the chosen forcing fields.

Finally, we have also carried out a month by month comparison of the SOC climatological wind stress fields with those derived in an earlier study by *May* [1982], who used ship reports over the period 1950-1970. We do not show the details but note that the circulation patterns in the two data sets are in good agreement except in February, when the northerly wind field over the Aegean is noticeably stronger in the SOC analysis than was found by *May*. The latter feature may be associated with anomalously intense late winter wind fields that occurred in the eastern Mediterranean in the early 1990s.

3. Model and Experiments

The model used is the Modular Ocean Model — Array (MOMA), a Bryan-Cox-Semtner type ocean general circulation model (OGCM) using the *Killworth et al.* [1991] free surface scheme. Besides the presence of the free surface, MOMA differs from the standard Geophysical Fluid Dynamics Laboratory (GFDL) MOM code [*Pacanowski et al.*, 1990] in that it is an array processor model, storing all variables in memory and thus not using the traditional slab structure. Revised horizontal and vertical advection schemes are also used in the baroclinic momentum equation. The model is described in greater detail by *Webb* [1993].

The model's governing equations are

$$\begin{aligned} \frac{\partial \mathbf{u}_h}{\partial t} + \mathbf{u} \cdot \nabla \mathbf{u}_h + f \mathbf{k} \times \mathbf{u}_h \\ = -\frac{1}{\rho_o} \nabla p - A_h \nabla^4 \mathbf{u}_h + A_v \frac{\partial^2 \mathbf{u}_h}{\partial z^2} \end{aligned} \quad (2)$$

$$\frac{\partial T}{\partial t} + \mathbf{u} \cdot \nabla T = -K_h \nabla^4 T + K_v \frac{\partial^2 T}{\partial z^2} \quad (3)$$

$$\nabla \cdot \mathbf{u} = 0 \quad (4)$$

$$\frac{\partial p}{\partial z} = -\rho g \quad (5)$$

$$\rho = \rho(\Theta, S, P_o) \quad (6)$$

where \mathbf{u} is the full velocity vector, \mathbf{u}_h is the horizontal velocity, f is the Coriolis parameter, \mathbf{k} is a vertical unit vector, T is a tracer (either potential temperature Θ , or salinity, S), p is the pressure, g is gravity, ρ is the den-

sity, and P_o is the pressure field calculated by integrating the hydrostatic equation using the reference density ρ_o only. Note that the equation of state in MOMA gives an in situ density.

The free surface model is an inviscid version of that of *Killworth et al.* [1991], as the lack of the viscous terms has been demonstrated to make little difference to the solutions [*Udall*, 1996]. To resolve the fast external gravity waves, the barotropic velocity fields and the free surface height are calculated using a small time step (60 s) with a larger time step for the baroclinic part of the model (3600 s). The barotropic pressure gradient is calculated directly from the gradient in sea surface height.

$$\frac{\partial h_o}{\partial t} = \frac{\partial(h_o u_o)}{\partial x} + \frac{\partial(h_o v_o)}{\partial y} \quad (7)$$

$$\frac{\partial u_o}{\partial t} = -\frac{\partial P_o}{\partial x} + f v_o + B_u \quad (8)$$

$$\frac{\partial v_o}{\partial t} = -\frac{\partial P_o}{\partial y} - f u_o + B_v \quad (9)$$

with

$$\frac{\partial P_o}{\partial x} = g \frac{\partial h_o}{\partial x} \quad \frac{\partial P_o}{\partial y} = g \frac{\partial h_o}{\partial y} \quad (10)$$

where h_o is the total ocean depth, u_o and v_o are the components of the barotropic velocity, P_o is the barotropic pressure, and B_u and B_v are the vertical-means of the baroclinic velocity tendencies (excluding the Coriolis term).

The model setup and formulation is based on the work of *Haines and Wu* [1995] and *Wu and Haines* [1996,1998]. Basin resolution is $0.25^\circ \times 0.25^\circ$ with 19 vertical levels. The bathymetry is that of *Wu and Haines* [1996]. The horizontal viscosity coefficient is $A_h = 3.0 \times 10^{18} \text{ cm}^4 \text{ s}^{-1}$ and the diffusion coefficient is $K_h = 1.0 \times 10^{18} \text{ cm}^4 \text{ s}^{-1}$. The vertical diffusion is $K_v = 0.3 \text{ cm}^2 \text{ s}^{-1}$ and the momentum diffusion is $A_v = 1.5 \text{ cm}^2 \text{ s}^{-1}$.

To handle the exchanges with the Atlantic, a small box is added outside of Gibraltar, where the temperature and salinity are relaxed on a 1-day timescale to the climatological values of *Levitus* [1982]. *Haney* [1971] relaxation conditions are applied at the surface for the tracers, using a modified surface data set based on National Oceanographic Data Center (NODC) data. The forcing repeats every year. The relaxation timescale for temperature is 2 hours (acting on a top layer of 10-m thickness), while it is 5 days for salinity, except in the Levantine, where it smoothly decreases to 2 hours east of 23°E . For a more detailed explanation on the choice of relaxation boundary conditions the reader is referred to *Wu and Haines* [1996]. Convective adjustment is performed using the complete convection scheme of *Rahmstorf* [1993]. The monthly varying wind stresses described in section 2 are used to force the model and are repeated every year.

Two series of experiments have been performed to examine the role that the different wind stress forcings

have on the circulation of the Mediterranean. In our first experiment we use the NMC-R wind climatology to spin up the model for 20 years. Except for the different model used (MOMA versus MOM) this is a repeat of the experiment of *Wu and Haines* [1996] and except where it is noted in the text, the results of the two models are similar. Some of the main differences between the results from the two different models (discussed further in section 5) are as follows: more freshwater transport through Gibraltar Strait in MOMA; a cleaner LIW pathway through Sicily Strait in MOMA; stronger Provencal gyre in MOM, and better Mersah-Matruh gyre in MOM. This experiment is repeated with three more 20-year runs (ECMWF, SOC, and NMC), using the ECMWF, SOC and NMC wind stresses.

This series of experiments allows us to compare the role that the different wind stresses have on the circulation in the Mediterranean. However, in all experiments, convection ceases in the Gulf of Lions within the first 10 years of the experiment, and a freshwater cap is formed. This is a common problem in many Mediterranean models [e.g., *Roussenov et al.*, 1995; *Wu and Haines*, 1996] although recent work with an improved sea surface temperature and salinity field may overcome this problem [*Wu and Haines*, 1998]. Since the collapsed western circulation is very different from what is observed, any intercomparison of the wind effects on the thermohaline circulation in the west is not going to provide much insight. A second series of experiments was performed to alleviate this problem, which will be discussed in section 5.4.

4. Heat and Freshwater Budgets

4.1. Observations

The semienclosed nature of the Mediterranean Sea makes it possible to estimate the heat transport through the Strait of Gibraltar, which may be equated (over a sufficiently long timescale that heat storage terms average to zero) to a surface flux over the entire basin. The flow through the Strait is essentially two layer, the upper layer consisting of a warm, fresh inflow from the Atlantic and the lower layer consisting of a cool, salty outflow. *Bethoux* [1979] considered the difference in the mean flow in the two layers and found a net heat inflow through the Strait equivalent to a heat loss over the basin of $7 \pm 3 \text{ W m}^{-2}$.

More recent measurements made in the Gibraltar Experiment [*Macdonald et al.*, 1994] have revealed the importance of an additional term in the heat transport equation, arising from correlations between velocity and temperature transients, which was not included in the earlier studies. These authors found values for the equivalent heat loss over the basin of 5.3 and 6.2 W m^{-2} utilising measurements made at two moorings situated in the centre of the Strait's main sill. However, they note that considerable uncertainties remain in the transport estimate arising from both the paucity

of measurements in the upper layer, which prevents a detailed estimate of the correlation term for the Atlantic inflow, and the short time span of the experiment, which prohibited any estimate of the effects of interannual variability and full resolution of the seasonal cycle. By combining data from other moorings in the Strait and the climatological atlas of *Robinson* [1971], they obtained a range of estimates of the equivalent net heat loss of $2.8 - 6.9 \text{ W m}^{-2}$, and this range is probably indicative of the minimum uncertainty in this value. Combination of measurements of the heat transport through the Strait of Sicily with those for Gibraltar allow average surface heat fluxes to be inferred separately for the eastern and western halves of the basin. Values inferred in this way are identical within the error range of the estimates, $5.7 \pm 7 \text{ W m}^{-2}$ for the western basin and $5.9 \pm 4 \text{ W m}^{-2}$ for the eastern [*Send et al.*, 1997].

Attempts to calculate the basin-averaged climatological heat flux using bulk formulae suffer from a greater range of error because of uncertainties in the parameterizations. In such studies the basin-averaged heat flux has tended to be a significant gain by the ocean rather than a loss, with typical values of $20 - 30 \text{ W m}^{-2}$ [*Bunker et al.*, 1982; *Garrett et al.*, 1993; *Gilman and Garrett*, 1994]. This is also the typical bias found on global scales [*Da Silva*, 1994] and is thus not just a Mediterranean problem, although the processes responsible for the bias may differ between the Mediterranean Sea and the global ocean. The emphasis has been on finding biases in the parameterizations which would allow the flux to be adjusted down toward the hydrographic value. Given these uncertainties, we focus on the hydrographic estimates (through Gibraltar and Sicily) for our evaluation of the model-implied heat fluxes.

Considering now the mean net freshwater flux over the basin, estimates of $E - P$ may be obtained via either the terrestrial or aerological branches of the hydrological cycle [*Gilman and Garrett*, 1994]. For the terrestrial analysis the net evaporation is given by the sum of river runoff into the basin and the freshwater flux in through the Strait of Gibraltar, while for the aerological analysis it can be equated with the divergence of the vertically integrated horizontal water vapor flux. *Gilman and Garrett* [1994] quote values of $E - P = 0.78$ and 0.66 m yr^{-1} from analysis of the terrestrial and aerological branches, respectively. Estimates may also be obtained from in situ climatologies, although these are sensitive to the choice of parameterizations used to calculate E and P . Preliminary analysis of the E and P fields in the SOC flux climatology gives a basin-averaged $E - P$ of 0.71 m yr^{-1} , between the aerological and terrestrial estimates discussed above.

4.2. Modelled fluxes

Surface fluxes of heat and freshwater in the model can be recovered from the *Haney* [1971] boundary con-

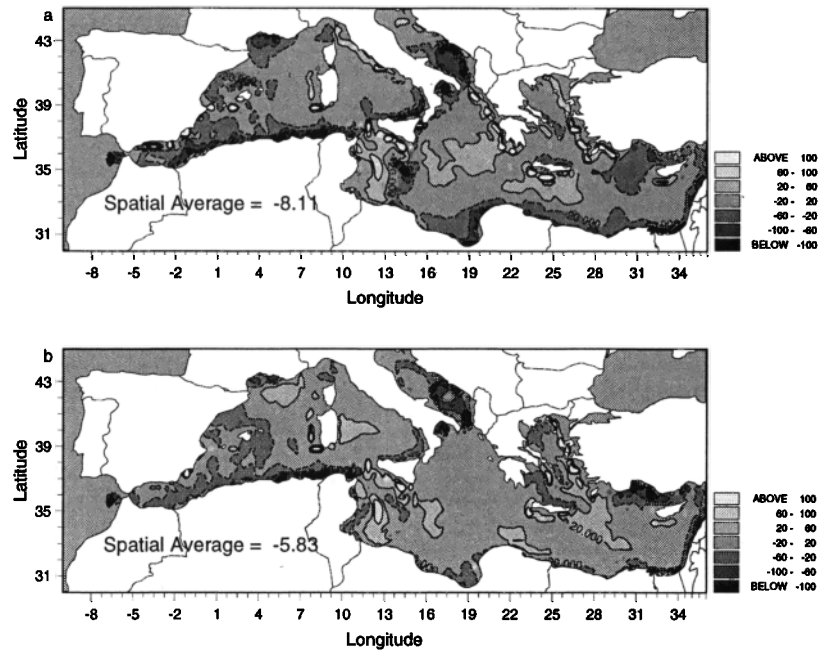


Figure 4. Annual average of surface heat fluxes ($W m^{-2}$): (a) NMC-R, (b) ECMWF, (c) SOC, and (d) NMC. Annual average of freshwater fluxes ($E - P$ $cm yr^{-1}$): (e) NMC-R, (f) ECMWF, (g) SOC, and (h) NMC.

ditions and used to calculate basin averages. The diagnosed surface heat flux and $E - P$ fields averaged over the last 5 years of each experiment are shown in Figure 4. The basin-averaged values, as well as averages over four subregions for each experiment, are listed in Table 2.

The basin-averaged heat flux in the SOC, ECMWF, and NMC experiments lie within the range of values found by *Macdonald et al.* [1994]. However, with the

unadjusted NMC-R wind stress fields a net loss of $8.1 W m^{-2}$ is found which lies just outside the measured range but probably within expected errors. The partition between the eastern and western basins in the model runs suggests similar heat losses in each basin, again in agreement with hydrographic measurements.

The heat flux maps show a band of enhanced heat loss along the African coast (note the large number of contours along the southern margin of the basin in Fig-

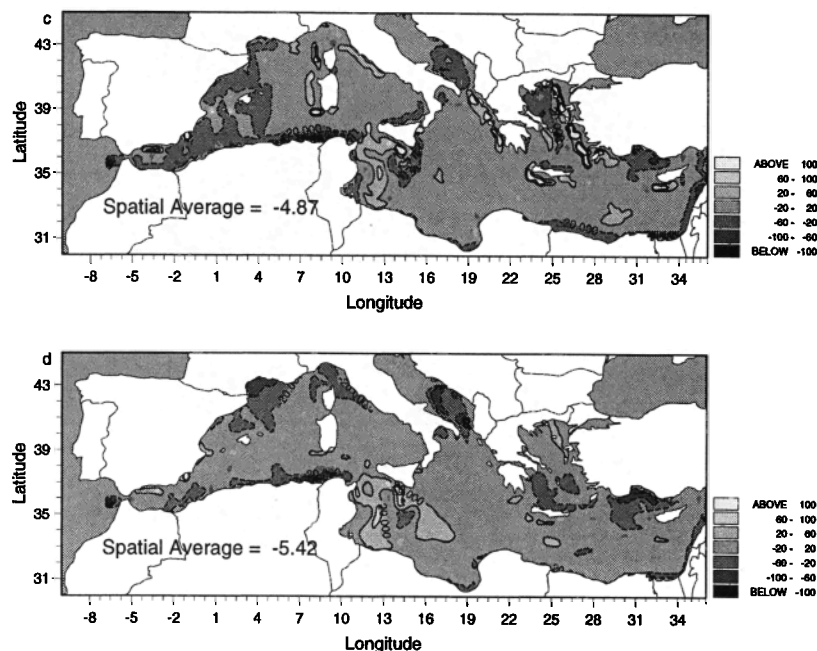


Figure 4. (continued)

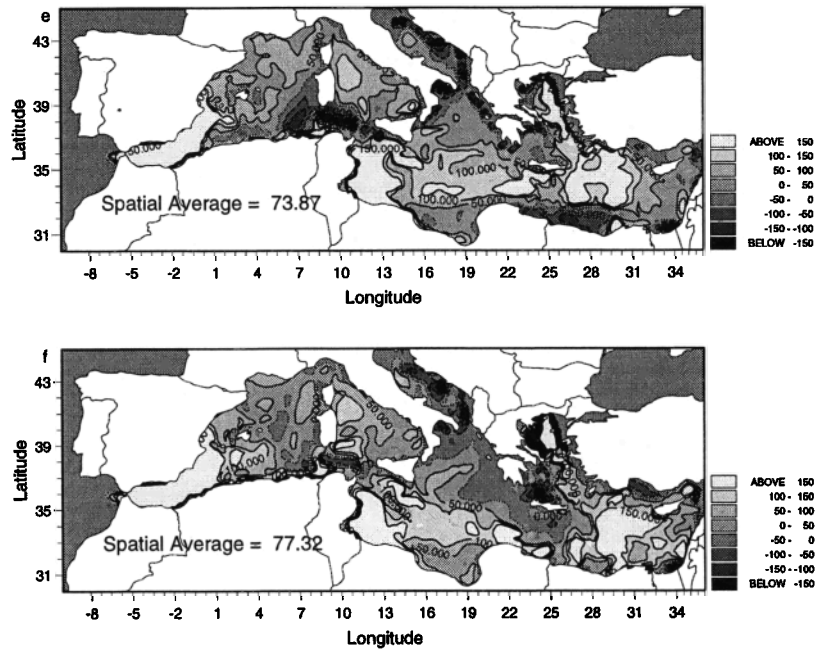


Figure 4. (continued)

ure 4a), as compared to the much sparser number of contours in Figure 4b-4d in the unadjusted NMC-R experiment that is not seen (or is much smaller) in response to the other forcing fields, including the NMC stresses. This feature is related to the strongly zonal NMC-R wind stresses, which produce excess upwelling of cold saline water along the basin's northern coast and downwelling of warm waters along the southern coasts. The upwelled water is warmed, resulting in blobs of surface heat gain along the northern boundaries in Figure 4a. Along the southern coasts the wind-induced downwelling pulls warm surface water toward the coast

by continuity, leading to the loss of more heat to the atmosphere, especially in winter. As the upwelling features are more localized than the downwelling (because of the NMC-R winds being less zonal in the northern basin and the irregular nature of the coastline), there is a greater net loss of heat in the unadjusted NMC-R experiment relative to the others. The assymetry between cooling and heating is also significant, with the downwelling along the African coast leading to thick mixed layers of warm water, which leads to a significant heat loss during early winter.

A further experiment was run from the end of the

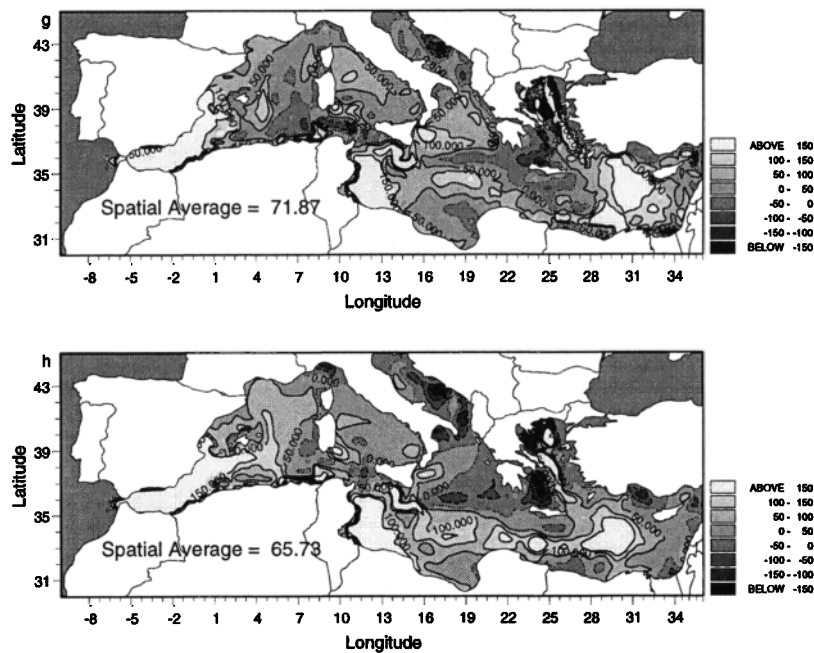


Figure 4. (continued)

Table 2. Surface Heat and Freshwater Fluxes for Our Basic Experiments and an Additional Experiment Where the NMC-R Winds Were Weakened by 20% (Described in Text)

Experiment	Heat Flux, W m^{-2}					E-P, cm yr^{-1}				
	MED	WMED	EMED	AD	AG	MED	WMED	EMED	AD	AG
NMC-R	-8.1	-10.9	-6.4	-37	-3.4	74	80	81	-47	-12
NMC-R \times 0.8	-5.0	-6.8	-4.7	-31	-9.4	70	85	77	-67	-63
ECMWF	-5.8	-9.4	-3.7	-46	-14.0	77	99	78	-42	-74
SOC	-4.9	-9.8	-2.0	-19	-22.3	72	87	73	-16	-7
NMC	-5.4	-11.3	-2.1	-30	-12.0	66	94	51	-39	-29

The regional abbreviations are MED, basin average; WMED, the western Mediterranean; EMED, the eastern Mediterranean (including the Adriatic and Aegean); AD, the Adriatic; AG, the Aegean, north of 36° (excepting the band of extreme warming and evaporation associated with the Bosphorus outflow).

NMC-R control run, for an additional 10 years, in which the wind stresses were uniformly multiplied by 0.8 to simulate the change expected from a more realistic drag coefficient. The band of heat loss associated with downwelling along the African coast decreases in extent, although it does not disappear entirely, and the basin-averaged heat loss is reduced to 5.0 W m^{-2} which is now within the observed hydrographic error range.

The model-derived basin-averaged $E - P$ values also lie within the observational range on large scales for all the fluxes over the western and eastern basins (MED, WMED, EMED in Table 2). However, there are wide differences in the modeled $E - P$ for the Adriatic (region AD) and the Aegean (region AG) when the different winds are used. Differences also show up in the heat fluxes over the Adriatic and Aegean. One would nat-

urally expect a greater sensitivity of smaller regions to the exact structure of the wind forcing; however, some of the differences are extreme, particularly when the SOC winds are used. Rather than discuss these in detail here we will leave the explanation to the following section, where differences in intermediate water circulation pathways, particularly in the eastern Mediterranean, are described.

5. Ocean Circulation

5.1. Surface Circulation

5.1.1. Western Basin. There is little difference in the Gibraltar transports (which range from 1.19 to 1.32 Sv) of Atlantic water into the Mediterranean. However, differences between the surface circulation ob-

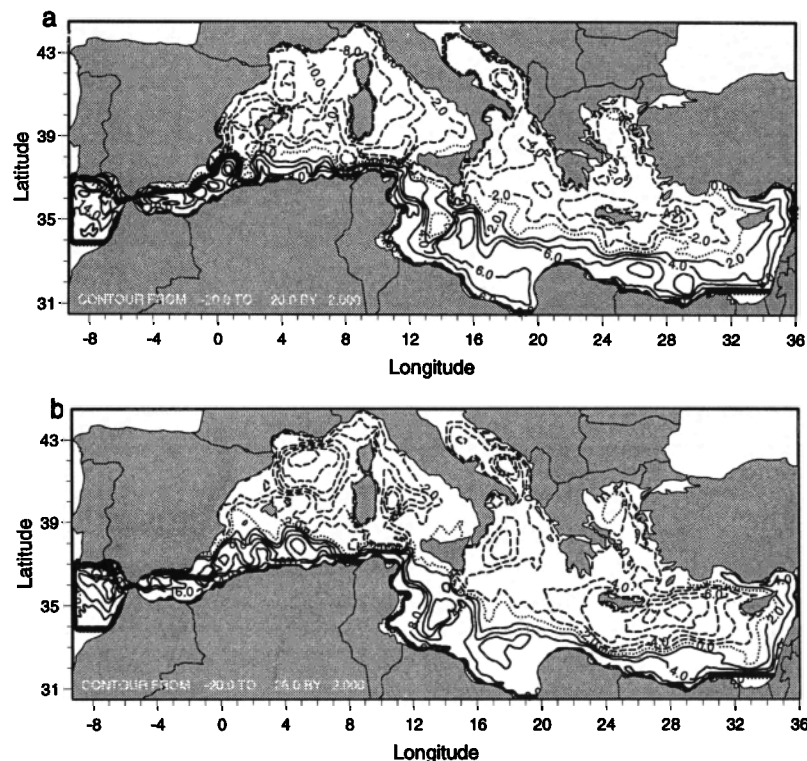


Figure 5. Annually averaged free surface height of: (a) NMC-R, (b) ECMWF, (c) SOC, and (d) NMC and (e) a schematic picture of the Mediterranean upper ocean structure (taken from Roussenov *et al.* [1995]).

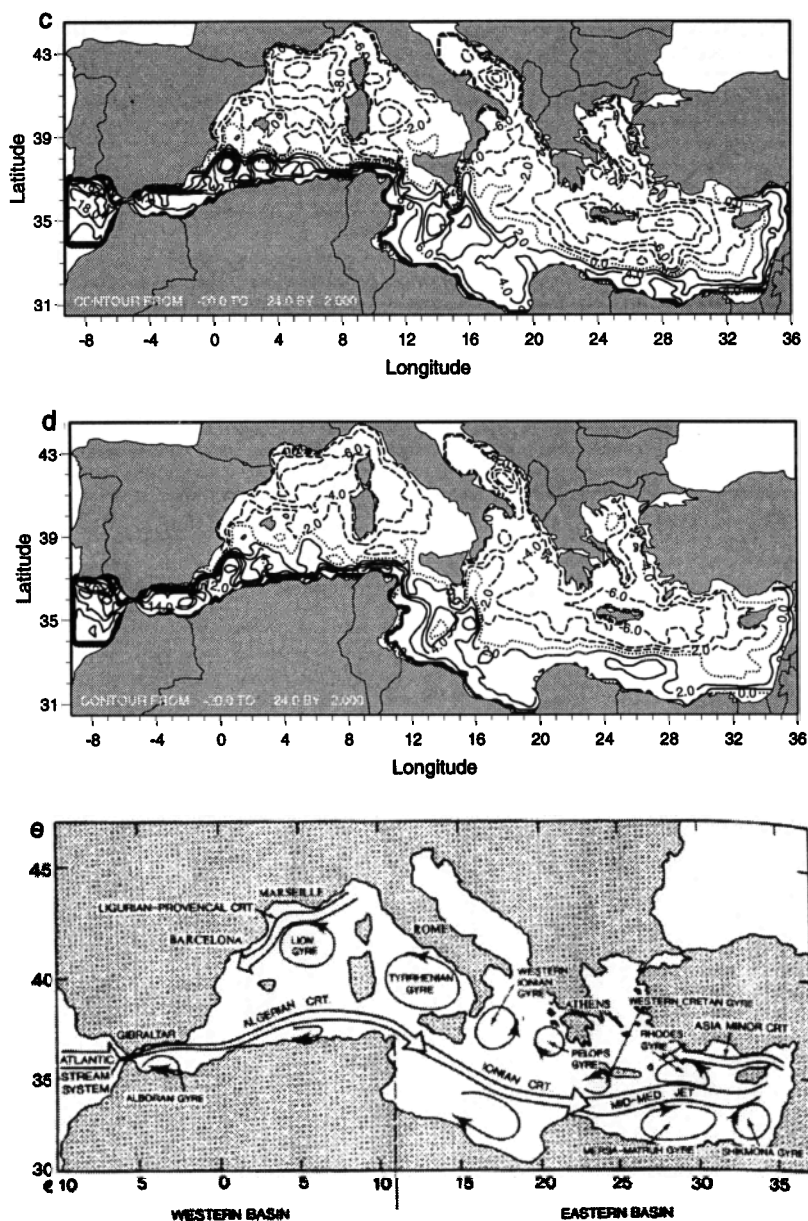


Figure 5. (continued)

tained from the wind stress fields are noticeable throughout the basin. The annually averaged free surface heights for the four runs are in Figure 5 and a schematic of the Mediterranean gyre structure, taken from Roussenov *et al.* [1995] is also shown in Figure 5e.

The flow that leaves the Alboran feeds the Algerian current. The current associated with the NMC-R winds has the least meandering and eddy shedding related to the zonality of the NMC-R winds in winter (meandering increases in summer from a winter minimum). It is also the tightest to the coast. Although initially near the coast, the ECMWF's Algerian current is very broad and far offshore, with a recirculation to the south (strongest in the autumn) along the eastern end of the Algerian coast. The situation in the SOC and NMC runs is intermediate to the other two, with SOC showing the most

meandering. In winter a distinct current may in fact not exist in the SOC run, with a series of eddies propagating down the coast.

All the wind stresses produce a cyclonic gyre in the Provencal Basin. The gyre is strongest with the ECMWF forcing and weakest under the NMC-R and NMC winds (Figure 5). In part this is related to the fact that under the NMC winds, only a very weak gyre exists in the summer/autumn (Thus the gyre is weak on an annual average. However, in winter it is significantly stronger than that associated with the NMC-R winds). Under the ECMWF winds the gyre is strongest in the late fall and early winter. This difference in strength plays an important role in the doming of the isopycnals for convective preconditioning, as shall be discussed in section 5.4.

The Tyrrhenian circulation is dominated by cyclonic flow, most visible in winter. Although this general pattern is reproduced with all wind stresses, a number of differences in structure are visible. The NMC and NMC-R winds drive the basic cyclonic flow and a broad northward flow along the Italian coast (which is strongest in winter). A much tighter and stronger cyclonic gyre is found off the Sardinian coast in the run under ECMWF forcing. The broad flow along the Italian coast is still present, but now there is also an anticyclone north of Sicily (in summer). This anticyclone (now present year round), and the basic cyclonic circulation, are maintained under the SOC forcing, but the northward current along the Italian coast has disappeared.

5.1.2. Eastern Basin. The flow through the Sicily Straits varies little between experiments (the range is 1.1 – 1.3 Sv), except NMC (0.9 Sv) on an annual average. In all cases the water leaving the Straits meanders northward around the Malta Rise. The meander is strongest under NMC-R forcing and weakest under ECMWF. There is also a strong seasonal dependence, with the meander most prominent in summer (except under the SOC forcing). This is the opposite to that found by *Zavatarelli and Mellor* [1995], who found a more complicated path in summer and little seasonality. This was a consequence of their use of the *May* [1982] forcing, which most resembles the SOC climatology. The behavior is similar in the NMC-R, NMC, and ECMWF cases, with a strong flow back to the south to drive an Ionian Current fairly directly across the southern part of the Ionian. However, with the SOC, no strong jet exists, with a series of weak currents and eddies flowing across the basin at a more northerly latitude than the current in the other experiments.

The Mid-Mediterranean Jet (MMJ) follows a fairly northerly path in the NMC-R run, as shown by *Wu and Haines* [1998], well off the Cyrenaican coast. It then bifurcates to the east of Crete, around 28°E. The northern branch flows north to feed a strong, tight, cyclonic Rhodes gyre. The southern branch flows across the central Levantine and around Cyprus to feed the Asia Minor Current. A small anticyclonic gyre (Shikmona) exists at the bifurcation point, which shifts east in winter. A large Mersah-Matruh gyre exists to the south of the MMJ. In the NMC experiment the MMJ is initially more southerly than NMC-R, but otherwise the behavior is similar, including a large Mersah-Matruh gyre.

In the ECMWF run the MMJ can be seen as a tight, vigorous current flowing along the African coast. Only a small, compressed Mersah-Matruh gyre exists to the south of the jet. The jet flows all the way to the eastern end of the basin, bifurcating south of Cyprus only. The jet is most stable in the summer, beginning to meander and shed eddies through the fall and into winter, when it is most unstable. Large-scale cyclonic circulation covers

both the Rhodes gyre and a large region southeast of Crete (Figure 5b).

Like the ECMWF case, the SOC winds drive the MMJ along a southern path close to the African coast. The strength of the jet shows more seasonal variability than under the other two forcings, with a distinct winter maximum. Instability and meandering is limited to the summer through autumn. Although still compressed, the Mersah-Matruh gyre is shifted to the east compared to the other experiments. The MMJ in the SOC run also bifurcates well into the eastern Mediterranean but much farther to the south than in the other experiments. The large cyclonic flow southeast of Crete is similar to that in the ECMWF experiment, but the gyre is weaker and not as deep (Figure 5c).

The strength of the cyclonic circulation in the Adriatic varies between experiments. It is much stronger and deeper under the ECMWF forcing than any of the other winds. The circulation also encompasses much more of the upper Adriatic in this run. It is weakest under the NMC stresses (which are the weakest in winter over the Adriatic) and drives very little circulation except in the lower Adriatic. Unlike the other cases, the SOC forcing drives a weak cyclonic circulation in the Aegean (Figure 5c). These differences may be indirectly affected by differences in the thermohaline circulation, which controls the Adriatic circulation. We will return to these two regions when we examine the changes in the intermediate and deep waters.

The NMC-R run produces a large Western Ionian gyre (in summer only, with a weak winter reversal) but no Pelops gyre off the Greek coast. This latter gyre is present under the NMC forcing, although it is weak. The ECMWF and SOC winds reproduce both of the above gyres (albeit more distinctly with the ECMWF forcing), as well as another small gyre between them. Associated with the NMC-R, NMC and ECMWF experiments are two anticyclonic gyres in the Gulf of Syrte. While the SOC forcing reproduces the westernmost of these gyres, the circulation in the central/eastern Gulf is cyclonic.

5.2. Intermediate Water Circulation

Intermediate water in the Mediterranean is dominated by Levantine Intermediate Water (LIW), a warm and salty water mass formed in the Rhodes gyre and Levantine. It plays a key role in the Mediterranean's thermohaline circulation by providing salty water to the deep water formation sites. Thus any changes in the formation or dispersal of this water mass, associated with the change in wind forcing, may have a significant effect on the basin as a whole.

There is little difference in the actual characteristics or formation rates of LIW between the experiments. As explained by *Wu and Haines* [1996], this is directly related to the fast restoring timescale used on salinity in the Levantine, which prescribes LIW formation to occur

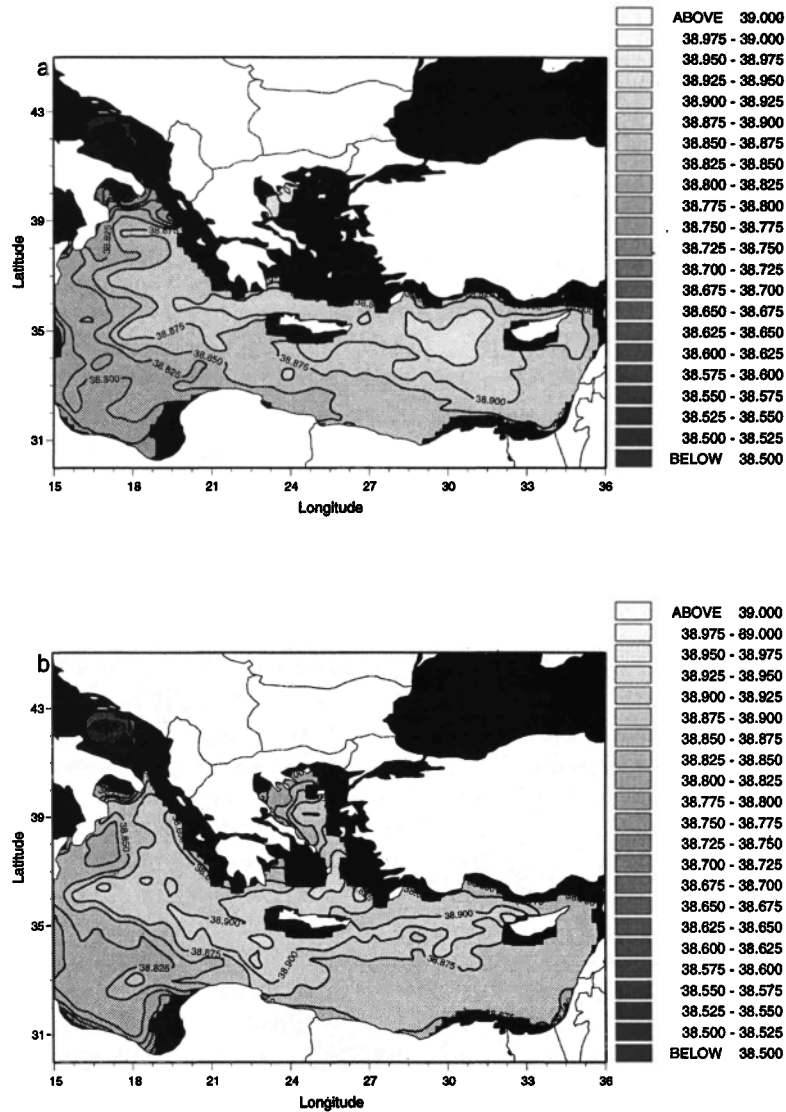


Figure 6. Annually averaged salinity (practical salinity units (psu)) along the 28.95 isopycnal: (a) NMC-R, (b) ECMWF, (c) SOC, and (d) NMC.

where it is observed. Without this procedure the model fails to produce an acceptable water mass, and there is then no hope of getting a reasonable thermohaline circulation for the Mediterranean. However, the longer salinity restoring timescale used elsewhere in the model permits an active role for salinity advection.

After LIW is formed and leaves the winter mixed layer, it spreads mainly on the 28.95 isopycnal. Since it is unforced except by diffusion, the properties should be nearly conserved on this isopycnal. As explained by *Wu and Haines [1996]*, salinity on an isopycnal surface makes a good tracer of dispersal pathways. Figure 6 shows the annual average of the model salinity on the 28.95 isopycnal for each experiment in the eastern basin. The initial dispersal of LIW is by baroclinic eddies, which do not appear in the annually averaged figures presented here. Instead, we show the overall pathways, the result of both mean flow and an ensem-

ble of the eddies. A change in wind stress can effect the intermediate water pathways in a number of different ways: (1) directly, with any changes in the strength and direction of the wind stress reaching down to mid-depths; (2) through the modification of surface currents and gyres that might act to block, redirect, or modify the intermediate currents flowing beneath them; and (3) through modification to the thermohaline circulation. Modifications to deep water production can act to increase or decrease the amount of intermediate water that must be transported to a site to compensate for the production of new dense water.

In all experiments the main pathway of LIW transport is west, toward the Ionian, mainly to the north of Crete. This is supported by observations from a 1995 cruise that the highest salinity water on these isopycnals can be found to the north of Crete [*Roether et al., 1998*], although *Wüst [1961]* suggests high salinities to

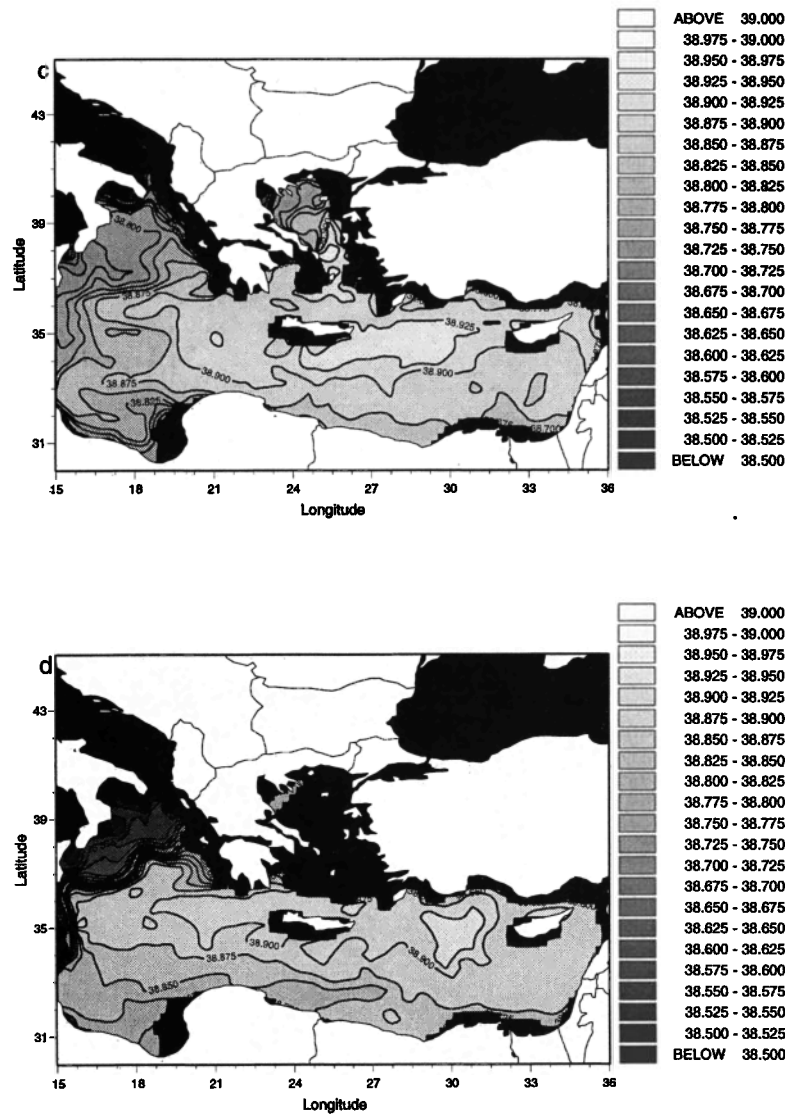


Figure 6. (continued)

the south of Crete as well. Under the SOC forcing (and somewhat under ECMWF and NMC) a significant component flows to the south of Crete (Figure 6). Both the NMC-R and SOC winds transport salty water into the eastern end of the Levantine, consistent with the observations, but this does not occur under the the NMC and ECMWF forcing (which may be related to the fact that the winds are both weak in this region and thus provide little assistance to the eastward transport of LIW by the baroclinic eddies).

There is very little flow (0.14 Sv) into or out of the Aegean (defined as the region north of 36°N) in the NMC-R and NMC runs. Note that we have chosen this latitude to be able to separate the mean transport of LIW toward the Ionian, which flows along the north coast of Crete in the model, from any actual LIW transport into the more northern parts of the Aegean. The amount of LIW flowing into the Aegean increases in the ECMWF experiment to 0.24 Sv. In both these

experiments, intermediate level inflow is balancing the outflow of surface water. Wind driven upwelling within the basin is probably responsible for a significant part of the exchange, but the Aegean also has negative $E - P$, so there is a possibility of lower density surface water outflow. However, the largest transport of LIW occurs under the SOC winds (0.35 Sv), with only part of this intermediate inflow being balanced by return flow at the surface. The rest is balanced by a deeper outflow. This is also associated with considerably greater cooling and less "precipitation" (i.e., smaller freshwater flux associated with the restoring boundary conditions) for the SOC experiment; see Table 2.

Associated with each of the wind stress fields is a different LIW pathway in the Ionian (Figure 6). In the NMC-R run, high-salinity LIW enters the northeast and central parts of the basin. The LIW decreases to the west and south. There is a significant flow of LIW along the Greek coast into the Adriatic. This changes

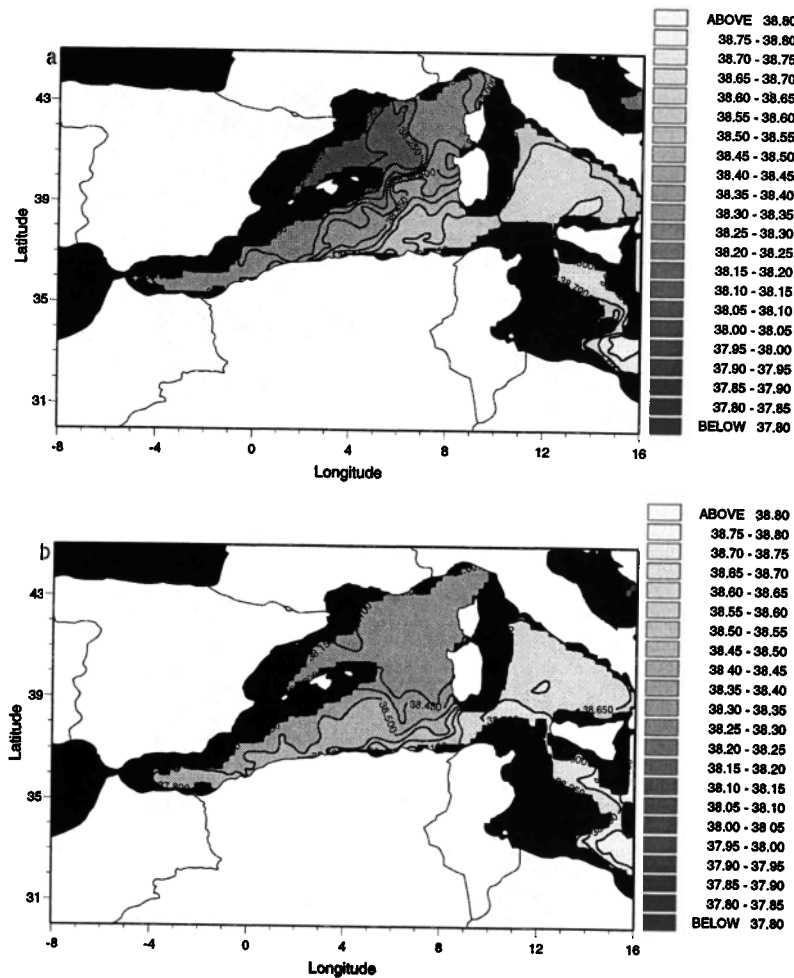


Figure 7. Annually averaged salinity (psu) along the following isopycnals: (a) 28.94 (NMC-R), (b) 29.00 (ECMWF), (c) 29.01 (SOC), and (d) 28.94 (NMC).

under the NMC stresses, with very low salinity water in the northern Ionian and a tongue of high-salinity LIW heading directly across the central Ionian to Sicily. In the ECMWF experiment, high-salinity, rather homogeneous water almost fills the entire central and northern Ionian. A decrease of salinity occurs moving to the south. Large amounts of LIW are transported into the Adriatic. The pattern associated with the SOC forcing is again the most distinct of all. Other than a narrow flow along the Greek coast, almost no LIW flows into the northern Ionian, and thus there is little transport into the Adriatic. The main core of LIW flows directly across the Ionian at the latitude of southern Sicily, and a very sharp front marks the northern boundary of this water mass (also seen in the NMC run). A tongue of LIW feeds the southern Ionian and the Gulf of Syrte (associated with the cyclonic gyre produced under this wind forcing). This middle Ionian pathway resembles that derived by *Wüst* [1961], using the core method.

Although all winds drive an LIW core through the Sicily straits, under the SOC and ECMWF winds the LIW is able to pass through the straits unchanged. However, under the NMC-R and NMC winds the 28.95

isopycnal is broken in the strait and, as found by *Wu and Haines* [1996], mixing decreases the LIW core to a density of 28.92, associated with the entrainment of warmer and fresher surface water. The LIW core sinks after entering the Tyrrhenian. This sinking is more pronounced in the MOMA model (under all wind stresses) than was found by *Wu and Haines* [1996] using the MOM model. As it sinks, the LIW core mixes with colder underlying water and increases in density. We now find that the LIW core south of Sardinia occurs on different isopycnals in each experiment: NMC-R and NMC, 28.94; ECMWF, 29.00; SOC, 29.01. The strong evaporative fluxes downstream from Sicily in the NMC-R experiment (Figure 4a) may be associated with the shallowness of the LIW in this experiment (with mixing leading to saltier surface waters).

Under the NMC-R and NMC wind fields (Figures 7a and 6d) the LIW path splits after it passes south of Sardinia, with a broad northward branch along the Sardinian/Corsican coast and a narrow southern branch along the Algerian coast. Both currents provide salt to the interior of the western basin by shedding eddies. Only the southern branch is present under ECMWF

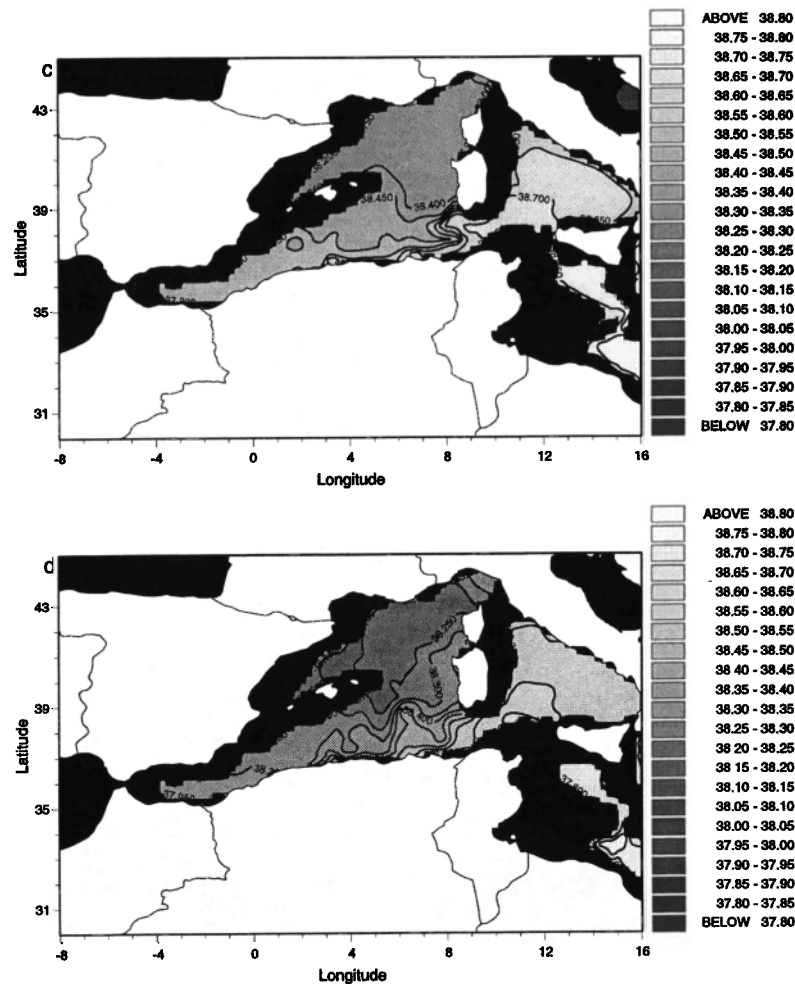


Figure 7. (continued)

(Figure 7b) and SOC (Figure 7c) forcing. In these later two experiments the salt that reaches the interior (at a salinity of 39.3 – 39.5 practical salinity units (psu)) is drawn into a broad, fairly deep (500 m) current in the interior that flows northeast toward Corsica and then feeds into the Ligurian-Provencal current. This brings the LIW to the Gulf of Lions, to provide salt for deep water formation.

5.3. Eastern Deep Water Formation

In the east, deep water is formed in the winter in the Adriatic through surface cooling and stirring combined with the entrainment of salty water from the underlying LIW layer. This newly formed water then flows out over the sill at Otranto to sink and fill the deeper parts of the eastern basin as Eastern Mediterranean Deep Water (EMDW). Changing the wind stress forcing in the model can affect this process in two ways: (1) changing of the strength of the cyclonic gyre in the lower Adriatic; (the doming of the isopycnals associated with Ekman suction affects the ease with which intermediate layer salt can be drawn into the convective event, permitting deepening) (2) the provision of LIW (and thus

salt) to the Adriatic, as described in section 5.2. This is crucial to the deep water formation process, for it is only with the availability of sufficient salt that water of sufficient density to sink to the bottom of the eastern Mediterranean can be formed in the Adriatic.

In terms of EMDW production the NMC-R and ECMWF experiments are similar. In both cases, adequate salt is provided to the Adriatic. The surface cooling is slightly enhanced in the ECMWF experiment, producing slightly colder deep water (13°C versus 13.25°C). The transports out through Otranto are also similar: 0.49 Sv in the NMC-R run (slightly larger than the 0.4 Sv found by *Wu and Haines* [1996]) and 0.55 for the ECMWF experiment. As the water sinks outside Otranto, it entrains the surrounding water. The exiting dense water undergoes excess mixing, and the associated decrease in density prevents the plume from reaching the bottom. *Haines and Wu* [1998] have shown that the *Gent and McWilliams* [1990] parameterization may improve this dense overflow problem. These experiments produce deep water with a density of 29.12 (NMC-R) and 29.13 (ECMWF) and a core salinity of 38.6 – 38.75 psu, centered at a depth of 1250 m (NMC-

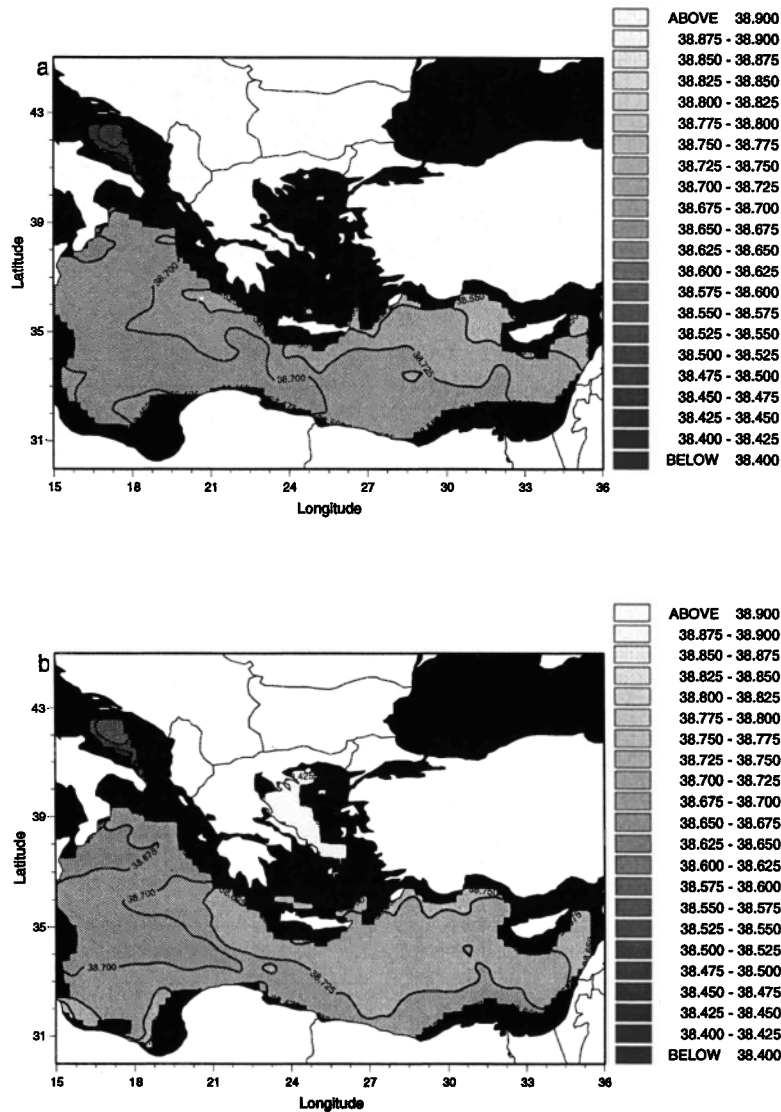


Figure 8. Annually averaged salinity (psu) along the following isopycnals: (a) 29.12 (NMC-R), (b) 29.13 (ECMWF), (c) 29.10 (SOC), and (d) 29.10 (NMC).

R) and down to 1600 m (ECMWF). The paths of this outflowing water are shown in Figure 8. An extended experiment, described in section 5.4, shows that over time, diffusion acts to increase the density of the EMDW to 29.16. This allows some EMDW to reach the bottom, although the main core remains higher up the water column.

Neither the SOC nor NMC winds transport large amounts of LIW into the northern Ionian and Adriatic, and thus convection in the Adriatic produces cold but fairly fresh (38.4 psu) water. The lack of intermediate saline water during convection can be seen in the reduced amount of P-E and smaller surface heat loss occurring over the Adriatic in this experiment (Figure 4c); see Table 2. Otranto transport is reduced to 0.32 Sv in the SOC experiment but not in the NMC run (0.44 Sv). With less warm saline LIW entering the Adriatic the surface water is already cooler and fresher,

and thus the restoring boundary conditions do not react as strongly. The deep Adriatic outflow is fresher (38.48 – 38.56 psu) and less dense (29.10) than in the other two experiments, and it is therefore shallower, with the core occurring at around 900 m. It also ventilates a much smaller and narrower band of the deep basin.

The decrease in Adriatic deep water production in the SOC experiment is compensated for by the production of high-salinity dense water in the Aegean. Figure 8c shows a tongue of high-salinity water stretching from the Aegean out to the north of Crete. This tongue is formed as a very salty (39.0 psu) and dense (in excess of 29.2) deep water mass in the lower Aegean that flows west toward the Ionian, descending as a gravity current down the continental slope. As it enters the Ionian, its density reduces to around 29.10, and it sinks to in excess of 750 m. The path also bifurcates, with a tongue flow-

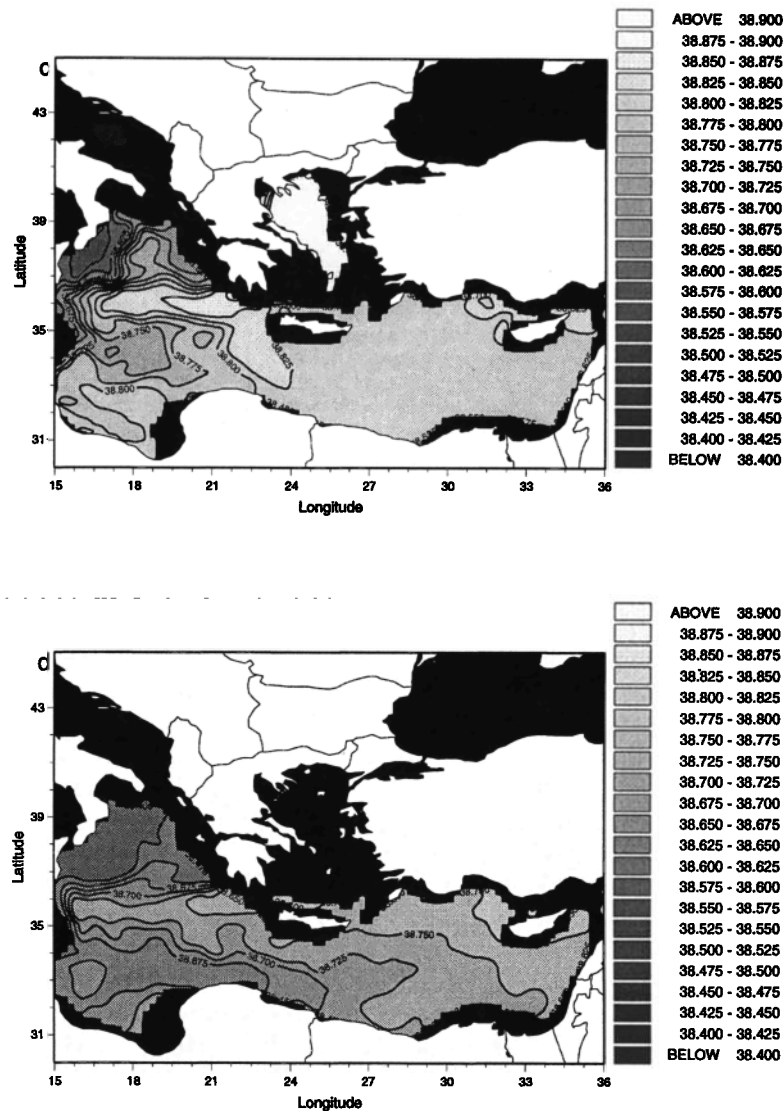


Figure 8. (continued)

ing directly across the Ionian, with high salinity (38.9 psu) and temperature ($> 14.4^{\circ}\text{C}$). The other branch flows south and east toward the African coast. As this Aegean water has very similar density to the Adriatic water, the southern tongue blocks the progress of Adriatic water toward the Levantine. Note that although the NMC experiment has a tongue in a similar region (Figure 8d), it is completely different in properties and origin. There, the water is not especially salty and consists of the older waters (standing out only because of the salinity differences with the very fresh EMDW surrounding it).

5.4. Western Deep Convection and Gibraltar Relaxation Experiments

With all our basic experiments we found that fresh water, inflowing at Gibraltar, pools in the western basin, acting to cap convection in the Gulf of Lions. In all cases, convection ceases within the first 10 years of in-

tegration. Four additional experiments (RELAX-NMCR, RELAX-NMC, RELAX-ECMWF, and RELAX-SOC) were therefore performed. In these experiments the relaxation to the *Levitus* [1982] climatology was extended through the Strait of Gibraltar to where it enters the Alboran Sea. The Strait of Gibraltar was also narrowed to 25 km (one grid point), although, perhaps surprisingly, this width change has little impact on the strait exchanges.

The imposition of the relaxation condition at Gibraltar acts to cut down the Gibraltar exchange flow, which is reduced to around 0.6 Sv in all experiments. This is achieved by reducing the N-S density gradient and hence the pressure gradient across the strait which controls the transports [Wadley and Bigg, 1996]. Fixing the water properties in the Strait only constrains the inflow/outflow (which we are not attempting to study here) and leaves the rest of the basin to respond freely. A disadvantage of this method is that limiting the salt

exchange through Gibraltar decreases the surface $E - P$ as the surface waters become, on average, more saline. Therefore we only use the RELAX series of experiments to examine the deep water formation in the western basin.

The RELAX-NMC-R experiment is run for 25 years, and we use year 15 of this experiment as the starting point for using ECMWF (RELAX-ECMWF) and SOC (RELAX-SOC) wind stresses, which were then integrated for a further 10 years. The RELAX-NMC experiment was integrated for 20 years from the initial conditions.

In all of the RELAX experiments, adequate salt is provided to the Provençal Basin, allowing the formation of Western Mediterranean Deep Water (WMDW) initially. However, the depth and intensity of convection is markedly different between the experiments. Under the NMC-R forcing, deep convection breaks down just after year 15, leaving only shallow temperature-dominated convection thereafter. In the RELAX-SOC experiment the circulation does not collapse, but deep convection occurs only sporadically. Otherwise, convection is to an intermediate depth. Deep convection occurs in all but one year in the RELAX-NMC experiment, with fairly fresh deep water being formed (38.29 psu). The RELAX-ECMWF run maintains vigorous and active deep convection. Therefore the RELAX-ECMWF run was extended for a further 100 years. The depth of the convection varies on both an interannual and interdecadal timescale, with shallow intermediate convection occurring in a few winters. WMDW is formed with a density of 29.06 and salinity of 38.32 psu and slowly spreads out to fill the deep western basin. The reason that deep convection continues throughout the RELAX-ECMWF run but not for the NMC-R or SOC winds is directly related to the strength of the Provençal gyre, where the weak stratification preconditions the system for convection. Convection continues in the RELAX-NMC experiment as the Provençal gyre, while weak on an annual average, is sufficiently strong in winter. The resulting deep water is fresher because less salt is provided to the region (Figure 7). To further illustrate the key role of the winds in preconditioning the system for convection, an additional experiment using the ECMWF wind stress field only and no surface forcing of T and S was performed. Although no deep water is formed, the ECMWF winds still produce strong doming of the isopycnals and weak stratification, implying that this is a wind-induced phenomenon and not a feature of the convection in this location.

6. Discussion and Summary

A series of experiments have been performed to examine the sensitivity of a Mediterranean OGCM to the choice of wind stress climatology. Significant differences exist between the climatologies chosen, three

of which have been compiled using output from numerical weather prediction models (NMC-R, NMC, and ECMWF) and one from in situ observations alone (SOC). We have chosen to use these climatologies because the NMC-R and ECMWF are in use by the Mediterranean modeling community; the NMC reanalysis illustrates the importance of *Roussenov et al.*'s [1995] choice of averaging for NMC-R, while SOC is similar to in situ climatologies [e.g. *May*, 1982] that have been used in past studies (in addition, it represents a new observational estimate of the climatological wind stress fields in this region over a recent period). There are some differences in the time periods covered by these climatologies, and we have not attempted to subset them for a particular time period. We have, however, performed several additional integrations (not shown) to verify that the results and differences highlighted in this paper are related to the differences in origin of the climatologies and not just to temporal differences.

The choice of wind stress climatology is found to have a number of effects on the model state. A number of the key differences are summarized in Table 3. The NMC-R winds are the most zonal of the data sets, this zonality relating to the the averaging procedure used by *Roussenov et al.* [1995] when generating the data set. We find our NMC climatology (from the NMC reanalysis) to be significantly less zonal, especially over the western Mediterranean in winter. *Wu and Haines* [1998], using NMC-R, found bands of heat gain/loss along the northern/southern coastal margins associated with Ekman transport and induced upwelling/downwelling, which also appear in the present study. With the other climatologies the boundary effects are reduced, while similar basin-averaged surface fluxes are found with all forcing fields. However, the position and strength of many of the gyres, currents and jets in the model do depend on the wind stress (e.g., Provençal gyre and circulation in the Tyrrhenian). The Ionian Current/MMJ shifts meridionally with different forcings and also bifurcates at different longitudes.

The dispersal pathways of Levantine intermediate water are altered by the winds. The ECMWF and NMC climatologies do not transport LIW into the eastern Levantine, possibly because of the weak winds in this region. In all cases the main LIW pathway is still to the west, toward the Ionian. Under the NMC-R forcing the majority of this transport occurs to the north of Crete, while substantial transport occurs to the south in the other runs. This may be associated with the different position of the MMJ in the different experiments. In the NMC-R run the MMJ occupies a northerly position, and the westerly flowing LIW recirculates back into the Levantine basin underneath the jet. In the other experiments the LIW pathway is unaffected by a more southerly MMJ. With the SOC climatology a significant transport of LIW into the Aegean occurs; consequently,

Table 3. Summary of the Main Similarities and Differences for the Model Forced by the Four Wind Stresses.

Circulation Feature	Experiment			
	NMC-R	NMC	ECMWF	SOC
Mistral Coastal	weak	strong	strong	strong
up,downwelling	yes	weak	weak	weak
Ionian Current	strong	strong	strong	weak
	southerly path	southerly path	southerly path	central path
MMJ	northern path	intermediate path	southern path	southern path
Mersah-Matruh gyre	strong	strong	weak	weak
LIW into Levantine	yes	no	no	yes
LIW past Crete	to north	some to south	some to south	split north/south
LIW in Ionian	north	central	north and central	central and south
LIW to Adriatic	yes	little	yes	little
EMDW formation Aegean	strong	intermediate, fresh	strong	weak, fresh
water formation	no	no	no	yes
WMDW formation	no	most years, fresh	yes	sporadic

MMJ, Mid-Mediterranean Jet; LIW, Levantine Intermediate Water; EMDW, Eastern Mediterranean Deep Water; WMDW, Western Mediterranean Deep Water. See the text for more details.

less LIW can pass on to reach the Adriatic, and hence, west of the Aegean, the LIW is confined mainly to the southern Ionian, resembling the distribution suggested by *Wüst* [1961].

A major result of this study is the sensitivity of EMDW formation to the wind stresses. Both the NMC-R and ECMWF runs transport LIW to the Adriatic and produce realistic amounts of EMDW. The core waters are slightly deeper and denser in the ECMWF experiment. With less LIW transported to the Adriatic in the NMC experiment the resulting EMDW is fresher and less dense. Similar results are seen in the SOC experiment, although here there is also a reduction in the amount of EMDW formed as well. One of the most intriguing features with the SOC winds is the production of a dense and salty intermediate/deep water mass in the Aegean, which has parallels in several observational studies. *Malanotte-Rizzoli and Hecht* [1988] review work from several authors that presents evidence for outflow into the Ionian from north of Crete at around 700 – 800 m. *Schlitzer et al.* [1991] note a high-salinity water mass between 500 and 1200 m in this region, with a source in the Aegean, which they denote as Cretan Intermediate Water (CIW). *El-Gindy and El-Din* [1986], in an examination of hydrographic data from 1948 to 1972, report deep Cretan Sea water, with a temperature of 14.2°C and 38.97 psu. These properties are very close to those of the Aegean outflow water produced here (compare section 5.3). Their plot of the percentage of deep Cretan water in the eastern basin at 2000-m depth (their Figure 13a) bears a remarkable resemblance to Figure 8c, showing two tongues of deep Aegean outflow in the Ionian and south of Crete. The shallowness of the Aegean outflow in the model may be

related to difficulties in representing model overflows at sills [see *Haines and Wu*, 1998].

Roether et al. [1996] recently reported that an influx of saltier water from the Aegean has replaced 20% of the bottom waters of the eastern Mediterranean. Associated with a sharp salinity increase in the Aegean since the late 1980s, Aegean deep waters have become saltier and denser and are now sinking to the bottom of the eastern Mediterranean. These authors speculate that this new deep water production is associated with a redistribution of salinity within the eastern Mediterranean, bringing increased amounts of LIW into the Aegean. This scenario is rather like that found here but on a much larger scale. The fact that we have found that dense water production is directly related to a change in the dispersal pathways of LIW supports the speculation of *Roether et al.* [1996] that the formation of Aegean deep water may be associated with a redistribution of salinity within the eastern Mediterranean. Although our model shows changes in surface fluxes associated with these changed water formation areas, the restoring boundary conditions prevent us from exploring freely the direct impact of variations in the surface fluxes on water formation sites.

Transport of LIW into the western basin occurs with all climatologies, although significantly greater mixing with surface waters occurs under the NMC-R and NMC winds. This, in turn, limits the sinking and associated density increase that occurs in the Tyrrhenian under NMC-R forcing. Further, with the NMC-R and NMC winds, there is a northern LIW pathway along Sardinia, in addition to the southern pathway along the North African coast found in the other two runs. In all cases, eddies transport salt from these boundary currents into

the interior, which is then provided to the Provençal gyre and the Gulf of Lions. However, it is the amount of wind-induced doming that occurs in the Gulf of Lions that determines whether deep convection occurs in this region. Under the ECMWF forcing the strong cyclonic circulation of the Provençal gyre allows sufficient salt to be entrained so that convection punches through to the bottom and WMDW is formed. A strong winter circulation with NMC winds allows deep convection too. The weaker gyre in the SOC experiment only allows for intermediate convection to occur in some years, while the almost complete lack of doming under the NMC-R winds causes a complete collapse of deep water formation once all the salt from the initial conditions is used up. In a model with more realistic boundary conditions the choice of winds would also play an important role through the advection of cold air off the continent and associated heat loss in winter.

In conclusion, we have examined our model forced by three different wind stress fields, derived from both observations and from numerical weather prediction models. Significant differences in the resulting model circulations exist which extend beyond the obvious wind-driven surface circulations to the pathways of the intermediate waters. By this means, the choice of wind stress forcing can affect the model's thermohaline circulation. We do not choose to recommend (or recommend against, other than the NMC-R climatology, which is highly suspect because of its averaging procedure) the use of any of these climatologies (NMC, ECMWF, and SOC) for ocean modeling studies, but we do note that significant changes can occur, especially in small regions like the Mediterranean, which depend critically on the winds used. The choice of wind stress may depend on what particular aspect of the Mediterranean's circulation is to be studied and which wind stress best reproduces that feature.

Acknowledgments. We would like to thank Peili Wu, Peter Taylor, and Margaret Yelland for helpful discussions and two anonymous reviewers for constructive comments. This work was primarily funded by the EU MAST CLIVAMP program under contract MAS3-CT95-0043. NCAR/NCEP reanalysis data was provided through the NOAA Climate Diagnostics Center (<http://www.cdc.noaa.gov/>). The SOC fields used in our analysis are part of a global climatological data set available via the web (<http://www.soc.soton.ac.uk/JRD/MET/fluxclimatology.html>). Permission to reproduce Figure 1 from *Malanotte-Rizzoli and Hecht* [1988] was given by Gauthier-Villars Editeur/ESME, 141 rue de Javel, 75747 Paris cedex 15.

References

- Beckers, J. M., *et al.*, First Annual Report: Mediterranean model evaluation experiment MEDMEX, Eur. Union Marine Science and Technology Program, Liège, 1996.
- Beckers, J. M., *et al.*, Second Annual Report: Mediterranean model evaluation experiment MEDMEX, Eur. Union Marine Science and Technology Program, Liège, 1997.
- Bethoux, J. P., Budgets of the Mediterranean Sea: Their dependence on the local climate and on characteristics of the Atlantic waters, *Oceanol. Acta*, **2**, 157-163, 1979.
- Bunker, A. F., H. Charnock and R. A. Goldsmith, A note on the heat balance of the Mediterranean and Red Seas, *J. Mar. Res.*, **40**, 73-84, 1982.
- DaSilva, A. M., C. C. Young and S. Levitus, *Atlas of Surface Marine Data 1994*, vol. 1, *Algorithms and Procedures*, NOAA Atlas NESDIS 6, 83 pp, Natl. Oceanogr. Data Cent., Silver Spring, Md, 1995.
- El-Gindy, A. A. H. and S. H. S. El-Din, Water masses and circulation patterns in the deep layer of the eastern Mediterranean, *Oceanol. Acta*, **9**, 239-248, 1986.
- Garrett, C., R. Outerbridge and K. Thompson, Interannual variability in Mediterranean heat and buoyancy fluxes, *J. Clim.*, **6**, 900-910, 1993.
- Gent, P. R. and J. C. McWilliams, Isopycnal mixing in ocean circulation models, *J. Phys. Oceanogr.*, **20**, 150-155, 1990.
- Gilman, C. and C. Garrett, Heat flux parameterizations for the Mediterranean Sea: The role of atmospheric aerosols and constraints from the water budget, *J. Geophys. Res.*, **99**, 511905134, 1994.
- Haines, K. and P. Wu, A modelling study of the thermohaline circulation of the Mediterranean Sea: Water formation and dispersal, *Oceanol. Acta*, **18**, 401-417, 1995.
- Haines, K. and P. Wu, GCM studies of intermediate and deep waters in the Mediterranean, *J. Mar. Syst.*, in press, 1998.
- Haney, R. S., Surface thermal boundary conditions for ocean circulation models, *J. Phys. Oceanogr.*, **1**, 241-248, 1971.
- Harrison, E. D., On climatological monthly mean wind stress and wind stress curl fields over the world ocean, *J. Clim.*, **2**, 57-70, 1988.
- Heburn, G. W., The dynamics of the seasonal variability of the western Mediterranean Sea, in *Seasonal and Interannual Variability of the Western Mediterranean Sea, Coastal Estuarine Stud.*, vol. 46, edited by P. E. La Violette, pp. 249-285, AGU, Washington, D. C., 1994.
- Hellerman, S., and M. Rosenstein, Normal monthly wind stress over the world ocean with error estimates, *J. Phys. Oceanogr.*, **13**, 1093-1104, 1983.
- Josey, S. A., E. C. Kent, D. Oakley, and P. K. Taylor, A new global air-sea heat and momentum flux climatology, *Int. WOCE Newsl.*, **24**, 3-5, 1996.
- Killworth, P. D., D. Stainforth, D. J. Webb, and S. M. Paterson, The development of a free-surface Bryan-Cox-Semtner ocean model, *J. Phys. Oceanogr.*, **21**, 1333-1348, 1991.
- Large, W. G., and S. Pond, Open ocean momentum flux measurements in moderate to strong winds, *J. Phys. Oceanogr.*, **11**, 324-336, 1981.
- Leviuts, S., Climatological Atlas of the world ocean, *NOAA Prof. Pap.* **13**, 173 pp., U.S. Gov. Print. Off., Washington, D. C., 1982.
- Madonald, A., J. Candela, and H. L. Bryden, An estimate of the net heat transport through the Strait of Gibraltar, in *Seasonal and Interannual Variability of the Western Mediterranean Sea, Coastal Estuarine Stud.*, vol. 46, edited by P. E. La Violette, pp. 249-285, AGU, Washington, D. C., 1994.
- Malanotte-Rizzoli, P., and A. Hecht, Large-scale properties of the eastern Mediterranean: A review, *Oceanol. Acta*, **11**, 323-335, 1988.
- May, P. W., Climatological flux estimates in the Mediterranean Sea, Part I, Winds and wind stresses, *NORDA Rep.* **54**, 57 pp., Nav. Ocean Res. and Dev. Activ., Stennis Space Center, Miss., 1982.

- Pacanowski, R. C., and K. Dixon, and A. Rosati, The GFDL Modular Ocean Model users guide, version 1.0, Geophys. Fluid. Dyn. Lab., Princeton, N. J., 1990.
- Pinardi, N., and A. Navarra, Baroclinic wind adjustment processes in the Mediterranean Sea, *Deep Sea Res. Part I*, **40**, 1299-1326, 1993.
- Rahmstorf, S., A fast and complete convection scheme for ocean models, *Ocean Modell.*, **101**, pp. 9-11, Hooke. Inst. Oxford Univ., Oxford, England, 1993.
- Robinson, M. K., R. A. Bauer, and E. H. Schroeder, Atlas of North Atlantic - Indian Ocean monthly mean temperatures and mean salinities of the surface layer, *Nav. Off. of Ref. Pub.*, **18**, Department of the Navy, Washington, D. C., 1979.
- Roether, W., B. B. Manca, B. Klein, D. Bregant, D. Georgopoulos, V. Beitzel, V. Kovacevuc, and A. Luchette, Recent changes in eastern Mediterranean deep waters, *Science*, **271**, 333-335, 1996.
- Roether, W., B. Klein, V. Beitzel, and B. B. Manca, Property distributions and transient-tracer ages in Levantine Water in eastern Mediterranean, *J. Mar. Syst.*, in press, 1998.
- Roussenov, V., E. Stanev, V. Artale, and N. Pinardi, A seasonal model of the Mediterranean Sea general circulation, *J. Geophys. Res.*, **100**, 13,515-13,538, 1995.
- Schlitzer, R., W. Roether, H. Oster, H.-G., Junghans, M. Hausmann, H. Johansen, and A. Michelato, Chlorofluoromethane and oxygen in the eastern Mediterranean, *Deep Sea Res. Part I*, **38**, 1531-1551, 1991.
- Send, U., G. Krahnmann, and C. Millot, Acoustic observations of heat content across the Mediterranean Sea, *Nature*, **385**, 615-618, 1997.
- Smith, S. D., Wind stress and heat flux over the ocean in gale force winds, *J. Phys. Oceanogr.*, **10**, 709-726, 1980.
- Stanev, E. V., J. J. Friedrich, and S. V. Botev, On the seasonal response of intermediate and deep water to surface forcing in the Mediterranean Sea, *Oceanol. Acta*, **12**, 141-149, 1989.
- Udall, I., The MOMA ocean general circulation model: An overview, U.K. Univ. Global Atmos. Modell. Programme Rep. 42, Bracknell, 1996.
- Wadley, M. R., and G. R. Bigg, Abyssal channel flow in ocean general circulation models with application to the Vema Channel, *J. Phys. Oceanogr.*, **26**, 38-48, 1995.
- Webb, D. J., An ocean model code for array processor computers, *Tech. Rep. 324*, Inst. of Oceanogr. Sci., Wormley, England, 1993.
- Woodruff, S. D., S. J. Lubker, K. Wolter, S. J. Worley, and J. D. Elms, Comprehensive Ocean-Atmosphere Data Set (COADS) release 1a: 1980-1992, *Earth Syst. Monit.*, **4**, 4-8, 1993.
- World Meteorological Organization, International list of selected, supplementary and auxiliary ships, *Tech. Rep. 1*, World Meteorol. Organ., Geneva, 1994.
- Wu, P., and K. Haines, Modeling the dispersal of Levantine Intermediate Water and its role in Mediterranean deep water formation, *J. Geophys. Res.*, **101**, 6591-6607, 1996.
- Wu, P., and K. Haines, The general circulation of the Mediterranean Sea from a 100-year simulation, *J. Geophys. Res.*, **103**, 1121-1135, 1998.
- Wüst, G., On the vertical circulation of the Mediterranean Sea, *J. Geophys. Res.*, **66**, 3261-3271, 1961.
- Yelland, M. J., B. I. Moat, P. K. Taylor, R. W. Pascal, J. Hutchings, V. C. Cornell, Wind stress measurements from the open ocean corrected for air flow disturbance by the ship, *J. Phys. Oceanogr.*, in press, 1998.
- Zavatarelli, M., and G. L. Mellor, A numerical study of the Mediterranean-Sea circulation, *J. Phys. Oceanogr.*, **25**, 1384-1414, 1995.

K. Haines and P. G. Myers, Department of Meteorology, University of Edinburgh, JCMB, Kings Buildings, Mayfield Road, Edinburgh, EH9 3JZ, Scotland, U.K. (email: kh@met.ed.ac.uk; paulm@met.ed.ac.uk)

S. Josey, James Rennell Division for Ocean Circulation, Southampton Oceanography Centre, Empress Dock, Southampton, SO14 3ZH, England, U.K. (email: Simon.A.Josey@soc.soton.ac.uk)

(Received May 19, 1997; revised November 18, 1997; accepted March 9, 1998.)